J Oral Pathol Med (2006) 35: 352–60

www.blackwellmunksgaard.com/jopm

Dual effect of nitric oxide in immortalized and malignant human oral keratinocytes: induction of apoptosis and differentiation

S-K. Lee[1], H-S. Kim[1], H-J. Lee[1], J. Lee[2], B-H. Jeon[3], C-D. Jun[4], S-K. Lee[5], E-C. Kim[1]

[1]*Department of Oral and Maxillofacial Pathology, College of Dentistry, Wonkwang University, Iksan, South Korea;* [2]*Department of Oral and Maxillofacial Surgery, College of Dentistry, Wonkwang University, Iksan, South Korea;* [3]*Department of Pathology, College of Oriental Medicine, Wonkwang University, Iksan, South Korea;* [4]*Department of Life Science, Gwangju Institute of Science of Technology, Gwangju, South Korea;* [5]*Department of Oral Pathology, College of Dentistry, Kangnung University, Kangnung, South Korea*

BACKGROUND: Nitric oxide (NO) is known to act cytostatically on several tumor cell when functioning as an effector molecule of activated macrophages, but the differential effects of NO on immortalized and malignant oral keratinocytes have not been examined.

METHODS: We investigated the influence of NO on the proliferation, cell cycle, apoptosis, and differentiation of immortalized human oral keratinocytes (IHOK) and primary oral cancer cells (HN4) using the 3-(4,5-dimethylthiazol-2-yl)-2,5-diphenyltetrazolium bromide (MTT) assay, sulforhodamine B (SRB) assay, flow cytometry, nuclear DNA staining, and Western blotting.

RESULTS: The MTT and SRB assays indicated inhibited growth of IHOK and HN4 cells that were treated with sodium nitroprusside (SNP) at concentrations higher than 1 mM but not at lower SNP concentrations. The higher concentrations of SNP up-regulated the apoptosis-related protein expression, which is consistent with the analyses of sub-G_1 phase arrest, annexin V-FITC (fluorescein isothiocynate) staining, nuclear staining, and DNA fragmentation. On the other hand, the lower concentrations of SNP enhanced the expression of keratinocyte differentiation markers in IHOK and HN4 cells.

CONCLUSIONS: These data suggest that high concentrations of NO can inhibit the growth of IHOK and HN4 cells through the induction of apoptosis, while low concentrations of NO can induce cytodifferentiation. The dual effects of NO, namely, the induction of apoptosis or cytodifferentiation, have important implications for the possible anti-oral cancer treatment.

J Oral Pathol Med (2006) **35**: 352–60

Correspondence: Associate Professor, Eun-Cheol Kim DDS PhD, Department of Oral and Maxillofacial Pathology, Dental College, Wonkwang University, Shinyoungdong 344-2, Iksan City, Jeonbuk, South Korea, 570-749. Tel.: +82 638 506 929. Fax: +82 638 507 351. E-mail: eckwkop@wonkwang.ac.kr
Accepted for publication February 16, 2006

Keywords: apoptosis; differentiation; growth; immortalized oral keratinocytes; nitric oxide; oral cancer

Introduction

Oral squamous cell carcinoma (SCC) is the most common cancer of the head and neck. Although oral cancer that is detected early is highly curable, more than 50% of oral cancer patients present with advanced disease, and fewer than 30% of these patients can be cured (1, 2). Studies during the past decade showed that concurrent chemoradiotherapy has the potential to improve the overall survival of patients with head and neck SCC (3). Thus, the continued investigation of new therapeutic agents is needed.

Nitric oxide (NO), a reactive nitrogen intermediate, is a short-lived free radical synthesized via the L-arginine to L-citruline pathway, which is mediated by nitric oxide synthase (NOS) in most animal cells. NO is involved in a large number of biological actions, but many of these processes are still poorly understood (4–6).

Moreover, it have demonstrated the potential of NO influence the proliferation and differentiation cascade in skin keratinocytes (7, 8). NO is generally considered to be an inducer of apoptosis in many cell types (9–13), but it protects other cell types from apoptosis (14, 15).

The NO and NO-related species have delineated antiproliferative, cytotoxic, and apoptotic effects of NO on several tumor cells, including leukemia, pancreatic, hepatic, and colon cancer (16–19). Although recently studies demonstrated NO-induced apoptotic effects on oral cancer cells (20, 21), comparative effects of proliferation and differentiation on oral immortalized vs. malignant keratinocytes cells towards NO was not reported.

In the present study, we demonstrated that NO caused growth inhibition of oral immortalized keratinocytes (IHOK) and oral SCC cell lines (HN4) primarily

by inducing apoptotic cell death. Additionally, we found that NO also stimulated the differentiation of both immortalized and malignant oral keratinocytes.

Materials and methods

Cell culture

HPV-immortalized human oral keratinocytes (IHOK) derived by transfecting normal human gingival epithelial cells with PLXSN vector containing the E6/E7 open reading frames of HPV type 16 (22), were selected using G418. The immortalized oral keratinocytes were cultured in the keratinocyte growth medium (KGM; Gibco, Grand Islands, NY, USA) supplemented with 2 ml of bovine pituitary extract (13 mg/ml), 0.5 ml each of hydrocortisone (0.5 mg/ml), human epidermal growth factor (0.5 μg/ml), insulin (5 mg/ml), epinephrine (0.5 mg/ml), transferrin (10 mg/ml), triiodothyronine (6.5 μg/ml), and GA-1000 and 0.05 mM $CaCl_2$.

HN4 (=HNSCC4) cells were cultured in Dulbecco's modified Eagle's medium (DMEM, Biofluid, Rockville, MD) containing 10% fetal bovine serum (FBS; Gibco) with 100 U/ml penicillin and 100 U/ml streptomycin (Life Technologies, Gaithersburg, MD). HN4 Cell line from a primary $T_3N_0M_0$ carcinoma of the mouth floor was derived in the laboratory of Dr John F. Ensley (Wayne State University) (23). All the cells were grown at 37°C in a humidified atmosphere of 5% CO_2 and 95% air. Cells were dissociated with 0.25% trypsin just before transfer for experiments and were counted using a hemocytometer.

Dulbecco's modified Eagle's medium (DMEM), KGM medium (Clonetecs), fetal bovine serum (FBS), and other tissue culture reagents were purchased from Gibco BRL (Grand Island, NY, USA). Anti-p16, p21, p53, pRb, bcl-2, bax, PCNA, CK6, CK16, CK19, and involucrin antibody were purchased from Santa Cruz (CA, USA) and cytochrome *c* antibody was obtained from PharMingen (San Diego, CA, USA). All other chemicals were obtained from Sigma Chemical (St Louis, MO, USA).

MTT cell viability assay

Viable cells were detected using 3-(4,5-dimethylthiazol-2-yl)-2,5-diphenyltetrazolium bromide (MTT) dye, which forms blue formazan crystals that are reduced by mitochondrial dehydrogenase present in living cells. Briefly, 2×10^4 cells were seeded in a 96 well plate and cultured overnight for cell attachment. Serial dilutions of NO were added, and cells were treated for 1, 3, and 5 days. After treatment, 50 μl of MTT solution (0.5 mg/ml in PBS) were added to each well and incubated for 4 h. To each well, 50 μl of DMSO were added. The plates were then shaken until the crystals had dissolved. Reduced MTT was then measured spectrophotometrically in a dual beam microtiter plate reader at 570 nm.

Sulforhodamine B (SRB) assay

The SRB assay was carried out as previously described (24). In brief, 70 μl 0.4% (w/v) sulforhodamine B (Sigma) in 1% acetic acid solution were added to each well and left at room temperature for 20 min. SRB was removed and the plates washed 5 times with 1% acetic acid before air drying. Bound SRB was solubilized with 10 mM unbuffered Tris-base solution (Sigma) and plates were left on a plate shaker for at least 10 min. Absorbance was read in a 96 well plate reader (Molecular Devices, Sunnyvale, CA, USA) at 492 nm subtracting the background measurement at 620 nm. The test optical density (OD) value was defined as the absorbance of each individual well, minus the blank value.

Flow cytometric analysis

Propidium iodide (PI) Staining

Cells (5×10^5) were cultured with or without SNP in medium containing 10% FBS in culture dishes at 37°C for 3 days. Cells were harvested, washed with PBS, fixed with 75% ethanol at 4°C for 2 h, then treated with 0.25 mg/ml of RNase A (Sigma Chemical Co) at 37°C for 1 h. After having been washed, the cells were stained with 500 μg/ml PI at room temperature for 10 min. Analysis was performed on flow cytometer (Beckton-Dickson, Franklin Lakes, NJ, USA). The percentage of cell in each stage of the cell cycle was determined by using the cell fit analysis program on the staining profile of viable cells.

FITC-annexin V and propidium iodine (PI) double staining

Phosphatidylserine translocation to the outer leaflet of the plasma membrane was assessed by reaction with Annexin V-FITC and detected by a FACScan flow cytometer. After treatments, 2×10^6 cells were harvested, washed with ice-cold PBS, and resuspended in 200 μl of binding buffer (10 mM HEPES/NaOH pH 7.4, 140 mM NaCl, 2.5 mM $CaCl_2$) and incubated with 5 μl of Annexin V conjugated with FITC for 10 min at room temperature in the dark. Samples were washed with binding buffer, resuspended in PBS, counterstained with 5 μg/ml PI, and then analyzed by flow cytometry to identify dead cells. Cells without treatment with SNP were used as a negative control. Cells showing up as Annexin V^-/PI^+ (Upper Left quadrant; UL) were recognized as necrotic, that showing up as Annexin V^+/PI^+ (Upper Right Quadrant; UR) were taken as late apoptotic or secondarily necrotic, whilst Annexin V^+/PI^- (Lower Right Quandrant; LR) cells were recognized as early apoptotic cells.

Morphological analysis of apoptosis by staining with DAPI

To confirm apoptosis by morphological observation, the cells were labeled with 2 μg/ml of the DNA dye, DAPI (Sigma), for 30 min at 37°C and visualized on a fluorescence microscope (Olympus, Tokyo, Japan). DAPI permeates the plasma membrane and yields blue chromatin. Viable cells display normal nuclear size and blue fluorescence, whereas apoptotic cells show condensed chromatin and fragmented nuclei.

Detection of DNA fragmentation by gel electrophoresis

Cell pellets (3×10^6 cells) were resuspended in 500 μl of lysis buffer (0.5% Triton X-100, 10 mM EDTA, and 10 mM Tris-HCl, pH 8.0) at room temperature for 15 min and centrifuged at 16 000 *g* for 10 min. DNA was then extracted using a Wizard genomic DNA

purification kit (Promega, Madison, WI, USA), precipitated with ethanol, and resuspended in Tris/EDTA buffer (10 mM Tris-HCL, pH 8.0, and 1 mM EDTA). DNA was analyzed after separation by gel electrophoresis (2% agarose).

Western blot analysis

For the Western blotting, stimulated cells were rinsed twice with ice-cold phosphate-buffered saline and then lysed in ice-cold lysis buffer [50 mM Tris-HCl, pH 7.4, containing 150 mM NaCl, 1% Nonidet P-40, 0.1% sodium dodecyl sulfate (SDS), 0.1% deoxycholate, 5 mM sodium fluoride, 1 mM sodium orthovanadate, 1 mM 4-nitrophenyl phosphate, 10 μg/ml of leupeptin, 10 μg/ml of pepstatin A, and 1 mM 4-(2-aminoethyl)benzenesulfonyl fluoride]. Cell lysates were centrifuged at 22 000 ***g*** for 20 min at 4°C, and the supernatant was mixed with a one-fourth volume of 4X SDS sample buffer, boiled for 5 min, and then separated through a 12% sodium dodecyl sulfate-polyacrylamide gel electrophoresis(SDS-PAGE). After electrophoresis, the proteins were transferred to nylon membranes using electrophoretic transfer. The membranes were blocked in 5% dry milk (1 h), rinsed, and incubated with secondary and primary antibodies (diluted 1:500–1:1000) in TBS for 1 h at room temperature. Finally, each protein was detected using an enhanced chemiluminescence system (Amersham Pharmacia Biotech, Piscataway, NJ, USA).

Evaluation of cytochrome c *release from mitochondria*

For the analysis of cytochrome *c* release from mitochondria, stimulated cells (1×10^7) were trypsinized and then washed with ice-cold buffer A (250 mM sucrose, 20 mM HEPES-KOH, 1 mM EDTA, 1 mM EGTA, 2 μg/ml leupeptin, 1 μg/ml pepstatin pH 7.4). Cells were resuspended in 200 μl of buffer A and carefully homogenized using a Dounce homogenizer. The homogenates were separated into cytosol (supernatant) and mitochondrial fractions (pellet) by differential centrifugation as described previously (25). Cytosolic proteins were then subjected to immunoblot analysis using the anti-cytochrome *c* monoclonal antibody as described above.

Results

Effects of SNP on cell growth by MTT and SRB assays

In order to compare the effects of NO on the growth of oral immortalized (IHOK) and malignant keratinocytes (HN4), exponentially growing cells were treated with an NO donor, sodium nitroprusside (SNP), and cell viability was evaluated by the MTT assay. The IHOK and HN4 cells that were treated with lower concentrations of SNP (0.05–0.2 mM) were free of cytotoxic effects after being cultured for 2 days, but showed decreased cell viability by 3 days. In contrast, cytotoxicity was readily apparent when these cells were treated with higher concentrations of SNP (0.75–3 mM). The growth of IHOK and HN4 cells was inhibited in a time- and dose-dependent fashion (Fig. 1a,b).

The SRB assay indicated that IHOK and HN4 cells showed an anti-proliferative effect after SNP treatment and that the effect gradually increased in a concentration-dependent manner, over the range of 1–3 mM SNP (Fig. 1c,d). The growth-inhibitory effect was not observed at SNP concentrations lower than 1 mM (Fig. 1c,d) in IHOK or HN4 cells.

Apoptosis induction by NO treatment

To elucidate whether the growth inhibitory effect of NO was attributable to the induction of apoptosis, cell cycle analysis, DNA fragmentation, DAPI staining, and flow cytometric analysis with annexin V/PI double-staining were performed. First, the cell cycle analysis of keratinocyte cells treated with 0.5–3 mM SNP for 2 days demonstrated a distinct, quantifiable population of cells with DNA content below the G_1 phase level (a sub-G_1 peak), indicating apoptotic cells. As shown in Table 1, the sub-G_1 fraction (hypodiploid DNA) increased in a concentration-dependent manner in both IHOK and HN4 cells, but IHOK cells were more sensitive to NO-induced cell cycle changes than HN4 cells. These flow cytometric data are consistent with the results of the MTT and SRB assays.

Second, the level of DNA fragmentation from the keratinocytes treated with 3 mM SNP for 48 h was assayed. After staining with ethidium bromide and visualization under UV light (Fig. 2a), DNA laddering indicative of apoptosis was observed in all IHOK and HN4 cells. The IHOK cells produced more abundant DNA ladders than did the HN4 cells. Third, a fluorescent DNA-binding dye, DAPI, was used to examine the nuclear morphology of dying cells. Cells treated with 3 mM SNP displayed typical morphological features of apoptotic cells containing condensed and fragmented nuclei (Fig. 2b).

Lastly, we examined the exposure of annexin V on the cell surface using annexin V/PI double-staining (Fig. 2c). Flow cytometric analysis revealed that the percentage of FITC-annexin V-positive but PI-negative cells that were apoptotic but not necrotic increased by more than 5% in IHOK cells treated with 3 mM SNP for 2 days. Collectively, these results indicate that high concentrations of NO induced apoptosis in immortalized IHOK and malignant HN4 keratinocytes.

Effects of SNP on the intracellular levels of cell cycle regulatory proteins, such as p53, $p21^{WAF1/CIP1}$, $p16^{INK4A}$, and Rb protein, by Western blot analysis

The IHOK cells showed increased expression of cell cycle regulatory proteins, such as p16, p21, Rb, and p53, depending on the SNP concentration. The expression was maximal at 0.5 or 0.75 mM SNP and gradually decreased at 1.0 or 2.0 mM SNP (Fig. 3a). These data suggest that the up-regulation of p53, p21, Rb, and p16 by SNP treatment is relevant to the inhibition of cell proliferation and the sub-G_1 arrest of IHOK cells.

As shown in Fig. 3b, the cell cycle regulatory protein expression in IHOK cells is different from that in HN4 cells after SNP exposure. In HN4 cells, the expression of p16 and p21 was not affected by treatment with 0.05–

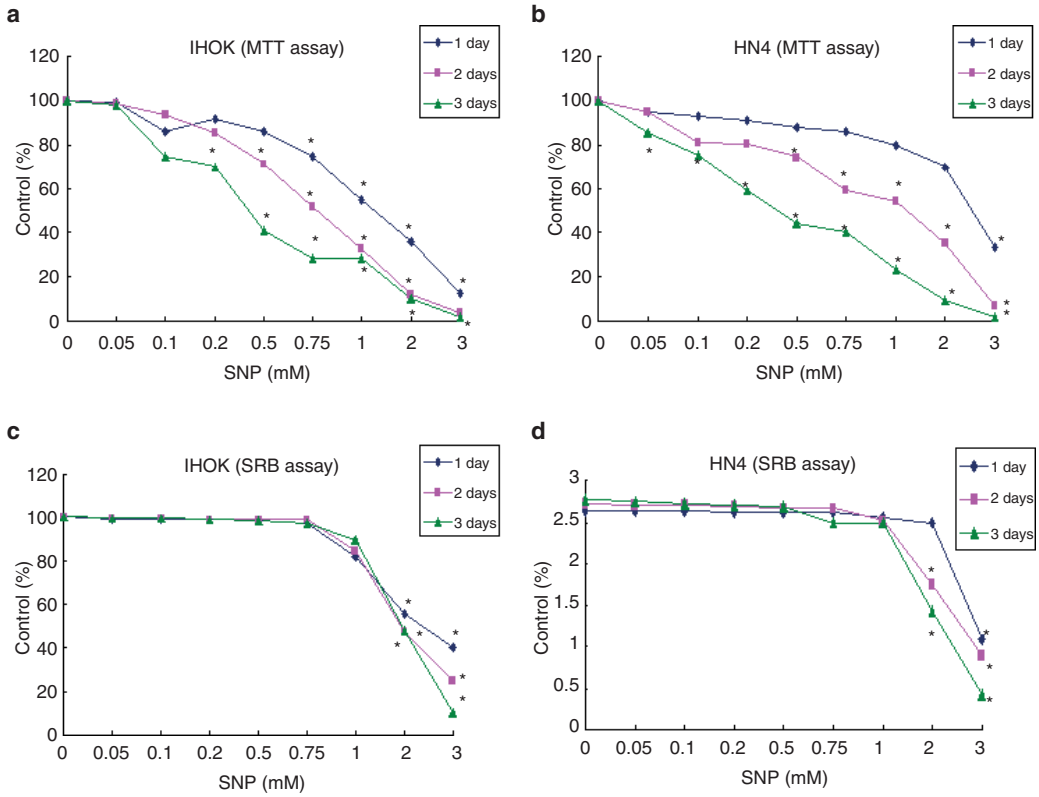

Figure 1 Effects of SNP on cell viability of immortalized human oral keratinocyte (IHOK, a and c), and primary oral cancer (HN4, b and d) cells as measured by MTT (a, b) and SRB assay (c, d). Each points and bar represent a mean ± SD. *Statistically significant difference compared with control group: $P < 0.05$.

Table 1 The effect of SNP on cell cycle distribution in immortalized and malignant oral keratinocytes

Cell line	*SNP*	*subG$_1$ (%)*	*G$_0$/G$_1$ (%)*	*S (%)*	*G$_2$/M (%)*
IHOK	Control	5.93 ± 2.71	68.22 ± 0.41	15.05 ± 1.16	7.51 ± 0.31
	0.5 mM	19.15 ± 3.32	41.27 ± 1.91	19.19 ± 1.46	7.85 ± 0.95
	1.0 mM	37.67 ± 5.3	44.2 ± 0.67	9.06 ± 1.09	5.28 ± 2.01
	2.0 mM	44.25 ± 0.33	44.22 ± 0.02	3.71 ± 0.05	4.24 ± 0.06
	3.0 mM	48.21 ± 0.56	45.5 ± 0.14	2.76 ± 0.16	2.18 ± 0.08
HN4	Control	1.74 ± 0.05	76.64 ± 0.79	5.1 ± 0.07	12.93 ± 0.28
	0.5 mM	2.4 ± 0.19	73.79 ± 0.8	4.97 ± 0.3	14.65 ± 0.35
	1.0 mM	4.28 ± 0.15	74.09 ± 0.89	6.06 ± 0.06	13.51 ± 1.06
	2.0 mM	14.95 ± 0.2	60.42 ± 0.58	7.08 ± 0.45	10.97 ± 0.01
	3.0 mM	25.54 ± 0.21	44.95 ± 0.72	15.74 ± 0.01	13.41 ± 0.12

These data are a mean ± SD of three independent experiments.

1.0 mM SNP for 48 h, but it decreased with 2.0 mM SNP. In HN4 cells, p53 and Rb were highly expressed with 0.1–0.75 mM SNP treatments. These findings suggest that exogenous NO was regulated in different manners depending on the NO concentration and cell type.

Western blot analysis of the intracellular levels of proliferation and apoptosis markers

To investigate the mechanism of NO-induced apoptosis in oral pre-malignant (IHOK) and cancer cells (HN4), we assessed the ability of NO treatment to modulate the expression levels of molecules involved in apoptotic signaling cascades (Fig. 4). In IHOK cells, the protein level of proliferating cell nuclear antigen (PCNA) markedly increased in a concentration-dependent manner over the range of 0.05–1.0 mM SNP, while the expression in HN4 cells remained unaltered even after treatment with 2.0 mM SNP.

We explored whether NO-induced apoptosis was related to a change in the expression of Bax and Bcl-2, because apoptosis might be regulated by the alteration of Bcl-2/Bax family protein expression. Western blotting showed that the up-regulation of Bax occurred at a low concentration of SNP (0.05 mM) in IHOK and HN4 cells and persisted at higher SNP concentrations (2 mM), but Bcl-2 was down-regulated at the highest

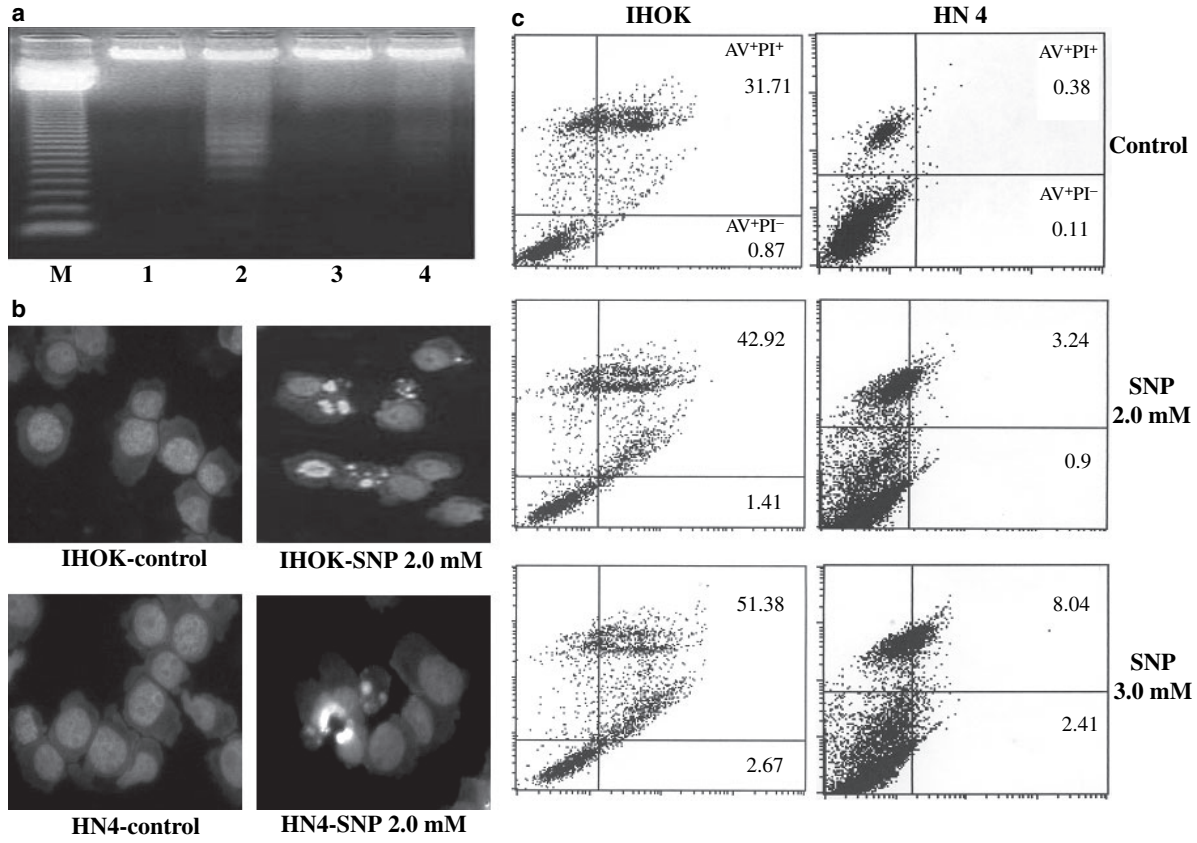

Figure 2 Confirmation of SNP induced apoptosis treatment in immortalized and malignant oral keratinocytes by DNA laddering (a), DAPI staining (b), Annexin V-PI flow cytometry (c). (a) DNA fragmentation was analyzed by 2% agarose gel electrophoresis (Lane 1, 2: IHOK, lane 3, 4: HN4, lane 1, 3: control, lane 2, 4: SNP treated). (b) Nuclear DAPI staining confirmation. 3.0 mM SNP for 2 days treated cells stained with DAPI. Stained nuclei were visualized under a fluorescence microscope (×200). (c) Representative Annexin V-PI flow cytometric analysis. Cells were incubated with 2 or 3 mM SNP for 2 days. And then they were stained with FITC-conjugated Annexin V and PI for flow cytometry.

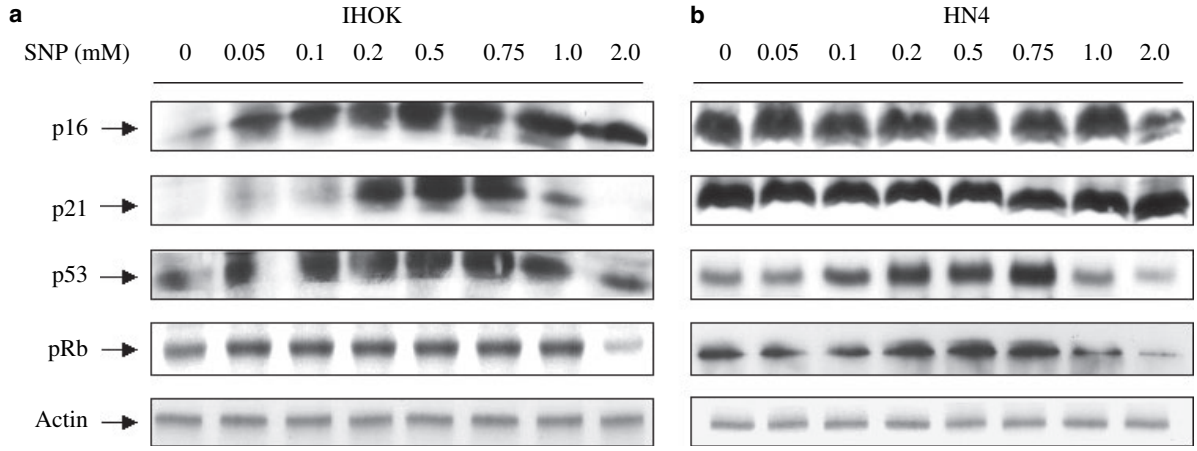

Figure 3 Western blot analysis of cell cycle regulatory protein expression such as p16, p21, p53 and Rb in IHOK (a), and HN4 (b) cells cultured without or with different concentration of SNP for 2 days. The protein fraction was extracted, electrophoresed, transferred to membrane and blotted with respective antibodies. These data are representative of three independent experiments.

SNP concentration (2.0 mM) in IHOK and HN4 cells. Moreover, we also discovered that procaspase-3 was activated by the SNP, but procaspase-8 was not activated in IHOK and oral cancer cells (data not shown).

Another cellular event that is associated with cell death is the release of cytochrome *c* from mitochondria (26). We used Western blot analysis to investigate whether mitochondrial cytochrome *c* was released into the cytosol. Treatment with NO resulted in cytochrome *c* release from the mitochondria into the cytosol after 2 days in IHOK and HN4 cells (Fig. 4). These data suggest that cytochrome *c* is a key factor in NO-induced

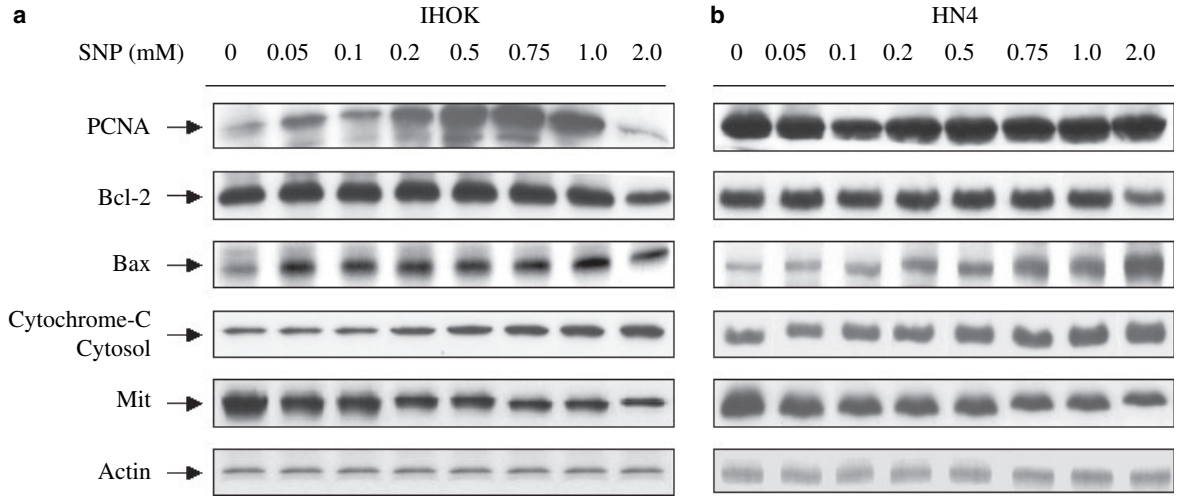

Figure 4 Western blot analysis of proliferation and apoptosis related protein expression such as PCNA, Bcl-2, Bax, and cytochrome-*c* in IHOK (a), and HN4 (b) cells cultured without or with different concentration of SNP for 2 days, and same procedure as described in the legend to Fig. 3 was performed.

apoptosis of IHOK and oral cancer cells, and its release may be correlated with the activation of caspase-3, which subsequently triggers the appearance of apoptosis.

Western blot analysis of intracellular levels of keratinocyte differentiation markers

The expression of involucrin, a protein precursor of the epidermal cornified envelope, and cytokeratins, epithelial-specific proteins, was examined in IHOK and HN4 cells after SNP treatment for 2 days. As shown in Fig. 5, SNP treatment induced the expression of keratinocyte differentiation markers, i.e. involucrin, CK 6, CK 13, and CK 19, in both IHOK and HN4 cells except high concentration of SNP (2.0 mM). The expression of these markers increased with increasing SNP concentration up to 1.0 mM SNP but markedly decreased at 2.0 mM SNP. Thus, both IHOK and HN4 cells showed increased expression of keratinocyte differentiation markers only at low or moderate concentrations of SNP, ranging from 0.05–1.0 mM.

Discussion

The NO is involved in cellular differentiation, proliferation and death and induces apoptosis in some cells or inhibits apoptosis in some cells. NO-induced apoptosis occurs in beta cells of the pancreas (27, 28), thymocytes (29), hepatocytes (30), and several other normal and immortalized cells (31–33). On the other hand, an antiapoptotic role of NO in some cultured cells has also been demonstrated. NO at low non-toxic concentration induces resistance to TNF α-induced hepatotoxicity (34), inhibits Fas-induced apoptosis in B lymphocytes (35), and modulates CD95-induced apoptosis in T-lymphocytes (36).

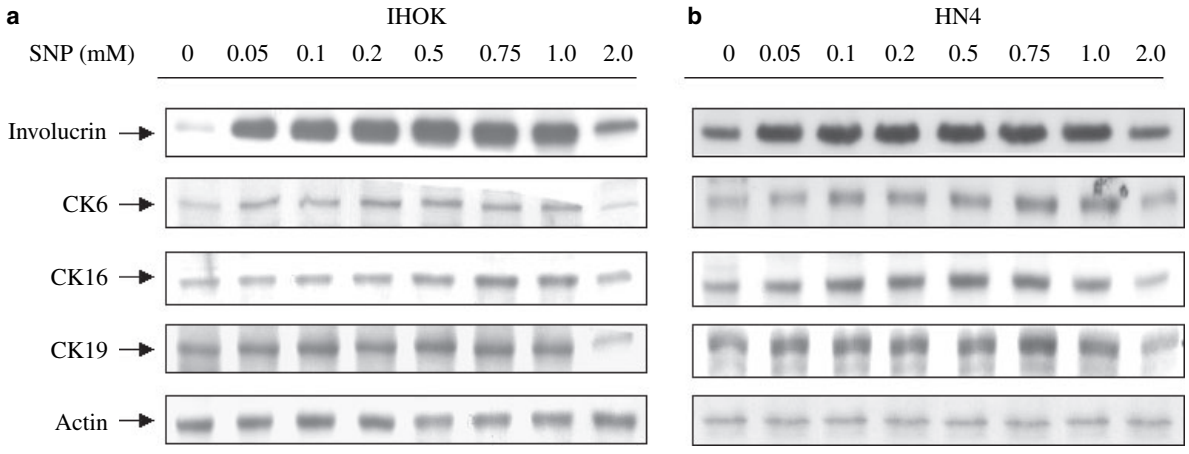

Figure 5 Western blot analysis of keratinocyte differentiation marker expression such as involucrin, cytokeratin (CK) 6, CK13, CK16 and CK 19 in IHOK (a) and HN4 (b) cells cultured without or with different concentration of SNP for 2 days and same procedure as described in the legend to Fig. 3 was performed.

Although previous studies have shown the effects of NO in leukemia and cancer cells, the effects of NO in oral immortalized and cancer cells were unknown. Therefore, we investigated the comparative effects of exogenous NO on the proliferation, cell cycle, apoptosis, and differentiation of HPV-IHOK and primary oral cancer cells (HN4).

In the MTT and SRB assays, the growth of IHOK and HN4 cells was found to be inhibited by concentrations of SNP higher than 1 mM (high concentrations), in a concentration- and time-dependent fashion, while IHOK and HN4 cells were relatively resistant to the cytotoxic and apoptotic effects of NO at low concentrations of SNP (0.05 and 0.1 mM). The SNP-induced growth inhibition was higher in IHOK cells than in HN4 oral cancer cells. Shang et al. (20), and Zhao et al. (21) found similar results, reporting that SNP exhibited concentration-dependent cytotoxicity and had no cytotoxicity against oral cancer cells until the SNP level exceeded 1 mM. This might be explained by the dual role of NO in carcinogenesis: a lower level of NO can promote the development and growth of tumor cells, while a higher, excessive level of NO may be noxious to tumor cells. This dual action of NO was recently found to be dependent on the local concentration of the molecules (20).

To study the mechanism of the anti-proliferative activity of NO, this study was focused mainly on determining whether NO possesses the potential to induce cellular apoptosis in immortalized and malignant oral keratinocytes. We demonstrated that NO, at cytotoxic millimolar concentrations, can trigger apoptosis in IHOK and HN4 cells. This notion is based on the following findings of this study: (i) Flow cytometric analysis showed that hypodiploid nuclei of IHOK and HN4 cells were increased after treatment with SNP (Table 1); (ii) IHOK and HN4 cells underwent internucleosomal DNA fragmentation (Fig. 2a) and morphological changes of the nucleus, which are characteristically noted in cellular apoptosis (Fig. 2b); (iii) FITC-annexin V and PI double-staining revealed that the apoptotic cell population, i.e. FITC-annexin V^+/PI^- cells, increased in IHOK and HN4 cells after exposure to a high concentration of NO (Fig. 2c).

To elucidate the mechanism by which NO inhibits the cell cycle progression of immortalized and malignant oral keratinocytes, we examined the cell cycle regulatory proteins that were affected by SNP treatment. As the SNP concentration increased from 0.05 to 1.0 mM, the levels of p53, p16, and $p21^{WAF1/CIP1}$ similarly increased in IHOK cells, but the levels of p16 and p21 were almost unchanged in HN4 cells. Thus, NO works in a biphasic manner in IHOK and HN4 cells by enhancing the expression of cell cycle regulatory proteins, i.e. p53 and pRb, at low SNP concentrations (0.05–0.75 mM) and conversely inhibiting cell growth at high SNP concentrations (1–2 mM).

Markers of DNA synthesis, such as Ki-67, and PCNA have been variably interpreted as indicators of cell regeneration and/or DNA repair (37). In our study, the increased expression of PCNA in IHOK cells and its stable expression in HN4 cells in response to SNP indicated that DNA repair or regeneration regulators may be activated to a greater degree in IHOK cells than in HN4 cells.

Increased expression of Bax may imply that a cell will undergo apoptosis by suppressing the activity of the Bcl-2 oncoprotein and related proteins, which play an important role in determining whether a cell will undergo necrosis or apoptosis (38). To elucidate the molecular mechanism underlying NO-induced cell death, apoptosis-regulated proteins were explored in IHOK and oral cancer cells treated with SNP for 48 h. It was consistently found that NO induced apoptosis of IHOK and HN4 cells through the up-regulation of Bax protein and downregualtion of Bcl-2.

The mechanism for caspase activation in apoptotic pathways is incompletely understood. Several studies suggest that cytochrome *c* release from mitochondria into cytosol in response to apoptotic stimuli may cause caspase activation (39). Cytosolic cytochrome *c* forms an essential part of 'apoptosome', which is composed of cytochrome *c*, Apaf-1 and procaspase-9. This complex results in activation of caspase-9, which then cleves and activates downstream executioner caspase-3 (40). Upon the treatment of IHOK and oral cancer cells, we noted the release of cytochrome *c* into the cytosol as well as the activation of caspase-3. On the contrary, there is no evidence of the activation of caspase-8. Moreover, the downregulation of Bcl-2, as well as the upregulation of Bax, coupled with the observed cytochrome *c* release, confirmed the mitochondrial dependent inherent in the NO-induced apoptosis of immortalized and malignant oral keratinocytes. The enhanced cytochrome *c* release into cytosol and the activation of caspase-3 but not caspase-8 in IHOK and oral cancer cells suggest that NO induces apoptosis in cells by mitochondrial dysfunction mechanism.

We examined whether NO was able to induce the differentiation of immortalized and malignant oral keratinocytes. Given the biphasic effect of NO, i.e. cytodifferentiation at low concentrations of NO and cellular apoptosis at high concentrations of NO, NO may directly regulate the essential processes of cell division and growth. It was reported that NO at higher concentrations enhances the expression of the differentiation marker CK6 in skin keratinocytes (13), while NO inhibits cornified envelope formation in human keratinocytes by inactivating transglutaminase (14). We also found that IHOK and HN4 cells treated with low and medium concentrations of NO (0.05–1.0 mM) showed increased expression of involucrin, CK6, CK16, and CK19, but the expression of the same proteins was decreased at high NO concentration (2 mM). We suggest that IHOK and HN4 cells respond to low concentrations of NO by undergoing the cytodifferentiation pathway of keratinocytes. In contrast, the cells cannot survive at high concentrations of NO and subsequently activate the cellular apoptotic cascade.

In summary, the present study revealed that NO has cytotoxic effects on immortalized and oral cancer

cells, causing them to undergo cytodifferentiation at low concentrations of NO and cellular apoptosis at high concentrations of NO. However, a clear distinction could be found between the immortalized keratinocytes and oral cancer cells. The latter were more resistant to the cytotoxic effects of exogenous NO than the former. We presume that the dual effect of NO is actually involved in the anti-cancer and pro-differentiation for immortalized and malignant oral keratinocytes, and that it may provide potential implication for the therapeutic use of NO in oral cancer and pre-neoplasia.

References

1. Marcus B, Arenberg D, Lee J, et al. Prognostic factors in oral cavity and oropharyngeal squamous cell carcinoma. *Cancer* 2004; **15**: 2779–87.
2. Vokes EE, Weichselbaum RR, Lippman SM, Hog WK. Head and neck cancer. *N Engl J Med* 1993; **328**: 184–94.
3. Pignon JP, Bourhis J, Domenge C, Designe L. Chemotheraphy added to locoregional treatment for head and neck squamous cell carcioma: three meta-analyses of updated individual data. MACH-NC collaborative group. Metaanalysis of chemotheraphy on head and neck cancer. *Lancet* 2000; **355**: 949–55.
4. Garthwaite J, Charles SL, Chess-williams R. Endothelium-derived relaxing factor release on activation of NMDA receptors suggests a role as intracellular messenger in the brain. *Nature* 1988; **336**: 385–8.
5. Furchgott RF, Zawadzki JV. The obligatory role of endothelial cells in the relaxation of arterial smooth muscle by acetylcholine. *Nature* 1980; **288**: 373–60.
6. Busse R, Mulsch A. Induction of nitric oxide synthase by cytokines in vascular smooth muscle cells. *FEBS Lett* 1990; **275**: 87–90.
7. Krishel V, Bruch-Gerharz D, Suscheck C, Kroncke KD, Ruzicka T, Kolb-Bachofen V. Biphasic effect of exogenous nitric oxide on proliferation and differentiation in skin derived keratinocytes but not fibroblasts. *J Invest Dermatol* 1998; **111**: 286–91.
8. Rossi A, Catani MV, Candi E, Bernassola F, Puddu P, Melino G. Nitric oxide inhibits cornified envelope formation in human keratinocytes by inactivating transglutaminase and activating protein 1. *J Invest Dermatol* 1998; **110**: 34–40.
9. Hajri A, Metger E, Vallat F, et al. Role of nitric oxide in pancreatic tumor growth: In vivo and in vitro studies. *Br J Cancer* 1998; **78**: 841–9.
10. Drapier JC, Wietzerbin J, Hibbs JB Jr. Interferon-gamma and tumor necrosis factor induce the L-arginine-dependent cytotoxic effector mechanism in murine macrophages. *Eur J Immunol* 1998; **18**: 1587–92.
11. Kröncke KD, Brener HH, Rodriguez ML, et al. Pancreatic islet cells are highly susceptible towards the cytotoxic effects of chemically generated nitric oxide. *Biochim Biophys Acta* 1993; **1182**: 221–9.
12. Sandau K, Brune B. The dual role of S-nitrosoglutathione (GSNO) during thymocyte apoptosis. *Cell Signal* 1996; **8**: 173–7.
13. Dimmeler S, Haendeler J, Nehls M, Zeiher AM. Suppression of apoptosis by nitric oxide via inhibition of interleukin-1 beta-converting enzyme (ICE)-like and cysteine protease protein (CPP)-32 like proteases. *J Exp Med* 1997; **185**: 601–7.
14. Li J, Bombeck CA, Yang S, Kim YM, Billiar TR. Nitric oxide suppress apoptosis via interrupting caspase activation and mitochondrial dysfunction in cultured hepatocytes. *J Biol Chem* 1999; **274**: 17325–33.
15. Shimuzu Y, Sakai M, Umemura Y, Ueda H. Immunohistochemical localization of nitric oxide synthase in normal human skin: expression of endothelial-type and inducible-type nitric oxide synthase in keratinocytes. *J Dermatol* 1997; **24**: 80–7.
16. Suitani K, Kamijo R, Nagumo M. Cytotoxic effect of sodium nitroprusside on cancer cells: involvement of apoptosis and suppression of c-myc and c-myb proto-oncogene expression. *Anticancer Res* 1997; **17**: 865–71.
17. Tsumori M, Tanaka J, Koshimura K, Kawaguchi M, Murakami Y, Kato Y. Cytotoxic effect of nitric oxide on human hematological malignant cells. *Acta Biochim Pol* 2002; **49**: 139–44.
18. Sokolowska M, Rokita H, Wlodek L. Activation of DNA biosynthesis in human hepatoblastoma HEPG2 cells by the nitric oxide donor, sodium nitroprusside. *Fundam Clin Pharmacol* 2003; **17**: 599–607.
19. Wenzel U, Kuntz S, De Sousa UJ, Daniel H. Nitric oxide suppresses apoptosis in human colon cancer cells by scavenging mitochondrial superoxide anions. *Int J Cancer* 2003; **20**: 666–75.
20. Shang ZJ, Li JR, Li ZB. Effects of exogenous oxide on oral squamous cell carcioma: An in vitro study. *J Oral Maxillofac Surg* 2002; **60**: 905–10.
21. Zhao SF, Tong XY, Zhu FD. Nitric oxide induced oral squamous cell carcinoma cells apoptosis with p53 accumulation. *Oral Oncol* 2005; **41**: 785–90.
22. Oda D, Bigler L, Lee P, Blanton R. HPV immortalization of human oral epithelial cells: a model for carcinogenesis. *Exp Cell Res* 1996; **226**: 164–9.
23. Cardinali MH, Pietraszkiewicz JF, Robbins KC. Tyrosine phosphorylation as a marker for aberrantly regulated growth-promoting pathways in cell lines derived from head and neck malignancies. *Int J Cancer* 1995; **61**: 98–103.
24. Kubota T, Takahara T, Nagata M, et al. Colorimetric chemosensitivity testing using sulforhodamine B. *J Surg Oncol* 1993; **52**: 83–8.
25. Thornberry NA, Lazebnik Y. Caspases: enemies within. *Science* 1998; **281**: 1312–6.
26. Yang J, Liu X, Bhalla K, et al. Prevention of apoptosis by Bcl-2: release of cytochrome *c* from mitochondria blocked. *Science* 1997; **275**: 1129–32.
27. Ankarcrona M, Dypbukt JM, Brune B, Nicotera P. Interleukin-1 beta induced nitric oxide production activates apoptosis in pancreatic RINm5F cells. *Exp Cell Res* 1994; **213**: 172–7.
28. Kaneto H, Fujii J, Seo HG, et al. Apoptosis cell death triggered by nitric oxide in pancreatic beta cells. *Diabetes* 1995; **44**: 733–8.
29. Fehsel K, Kroncke KD, Meyer KL, Huber H, Wahn V, Kolb-Bachofen V. Nitric oxide induces apoptosis in mouse thymocytes. *J Immunol* 1995; **155**: 2858–65.
30. Kim YM, Bergonia H, Lancaster JR. Nitrogen oxide-induced autoprotection in isolated rat heaptocytes. *FEBS Lett* 1995; **374**: 228–32.
31. Suenobu N, Schchiri M, Iwashina M, Marumo F, Hirata Y. Natriuretic peptides and nitric oxide induce endothelial apoptosis via a cGMP-dependent mechanism. *Arterioscler Thromb Vasc Biol* 1999; **19**: 140–6.
32. Battinelli E, Loscalzo J. Nitric oxide induces apoptosis in megakaryocytic cell lines. *Blood* 2000; **95**: 3451–9.

33. Taimor G, Hofstaetter B, Piper HM. Apoptosis induction by nitric oxide in adult cardiomyocytes via cGMP signaling and its impairment after stimulated ischemia. *Cardiovasc Res* 2000; **45**: 588–94.
34. Kim YM, De Vera ME, Watkins SC, Billar TR. Nitric oxide protects cultured rat hepatocytes from tumor necrosis alpha-induced apoptosis by inducing heat shock protein 70 expression. *J Biol Chem* 1997; **272**: 1402–11.
35. Mannick JB, Miao XQ, Stamler JS. Nitric oxide inhibits Fas-induced apoptosis. *J Biol Chem* 1997; **272**: 24125–8.
36. Sciorati C, Rover P, Ferranini M, Heltai S, Manfredi AA, Climenti E. Autocrine nitric oxide modulates CD95-induced apoptosis in gamma delta T lymphocytes. *J Biol Chem* 1997; **272**: 23211–5.
37. Studillo H, Lopez T, Castillo S, Gariglio P, Benitez L. p53, Bcl-2, PCNA expression, and apoptotic rates during cervical tumorigenesis. *Ann N Y Acad Sci* 2003; **1010**: 771–4.
38. Oltvai ZN, Miliman CL, Korsmeyer SJ. Bcl-2 heterodimeized in vivo with a conserved homolog, Bax, that accelerates programmed cell death. *Cell* 1993; **74**: 609–19.
39. Green DR, Reed JC. Mitochondria and apoptosis. *Science* 1998; **l28**: 1309–12.
40. Li P, Nijhawan D, Buduhardjo L, et al. Cytochrome *c* and dATP-dependent formation of Apaf-1/caspase-9 complex initiates an apoptoic protease cascade. *Cell* 1997; **91**: 479–89.